

H of 60 mm, mean diameter D_{50} of 0.21 mm, and uniform coefficient U_c of 1.70.

Reinforced roadbeds were introduced in Cases 3 and 4. A Toyoura sand roadbed ($D_r = 90\%$, $H = 60$ mm) was overlain by an asphalt mixture layer in Case 3, and a Natom sand roadbed ($D_r = 95\%$, $H = 60$ mm) was overlain by the same asphalt mixture layer in Case 4. The D_{50} of the Natom sand was 0.70 mm, and its U_c was 3.09. The 10 mm thick asphalt mixture was composed of straight asphalt 80–100 and sands.

Table 1. Model ground conditions

Case No.	Roadbed	Ballast thickness H_b (mm)
1	1-1 Steel (Bottom plate of a sand box)	20
	1-2	50
	1-3	80
2	2-1 Toyoura sand ($D_r = 90\%$, $H = 60$ mm)	20
	2-2	50
	2-3	80
3	3-1 Toyoura sand ($D_r = 90\%$, $H = 60$ mm) + Asphalt mixture (layer thickness = 10 mm)	20
	3-2	50
	3-3	80
4	4-1 Natom sand ($D_r = 95\%$, $H = 60$ mm) + Asphalt mixture (layer thickness = 10 mm)	20
	4-2	50
	4-3	80

Cyclic loadings were applied to the model grounds with footing at a constant displacement rate of 0.05 mm/s. The amplitude of the cyclic stress applied in Case 1 was 110 kN/m²; that applied in Cases 2, 3, and 4 was 80 kN/m². During the cyclic loadings, consecutive images of the model grounds were captured by a digital camera.

In each test, 100 cyclic loadings were first applied. Tie-tamper repair modeling was performed in the following manner. As shown in Fig. 2, the footing was reset to the initial position after 100 cyclic loadings were applied. A small spoon was next inserted into the model ground near lateral sides of the footing. After the spoon reached a fixed ground depth, it was tilted several times to permit the crushed stones to move laterally. This procedure was followed at several locations until the voids between the footing and the ground surface were completely filled by the crushed stones. Finally, additional crushed stones were introduced to the ground surface near the footing sides to produce a flat ground surface. After this tie-tamper modeling was implemented, 100 of cyclic loadings were applied again.

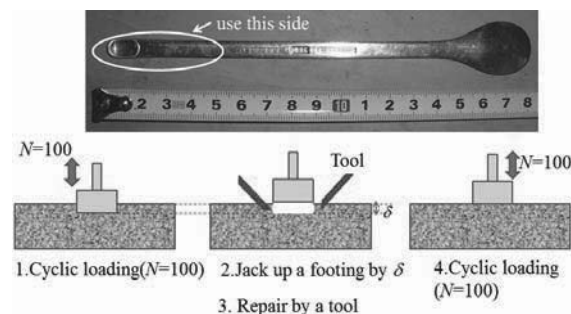


Figure 2. Tool and procedure used for simulating tie-tamper repair

3 RESIDUAL DEFORMATION CHARACTERISTICS

3.1 Effects of ballast thickness

The relationships between the number of cyclic loadings N and footing settlement δ were obtained before and after tie-tamper repair, as shown in Fig. 3. Each relationship obtained could be fitted by the following equation²⁾:

$$\delta = C(1 - e^{-\alpha N}) + \beta N \quad (1)$$

where C and α are parameters representing the initial settlement process, and β represents the process of gradual subsidence.

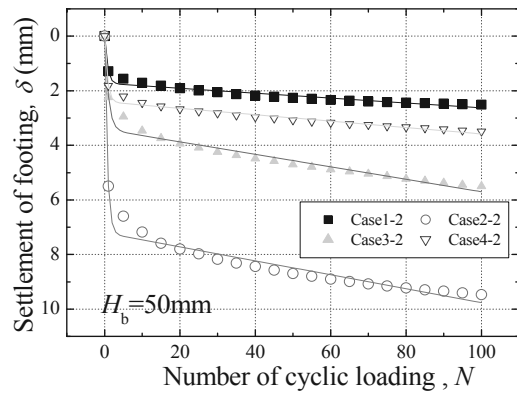


Figure 3. Relationships between number of cyclic loading cycles and footing settlement before tie-tamper implementation. Ballast thickness, $H_b = 50$ mm

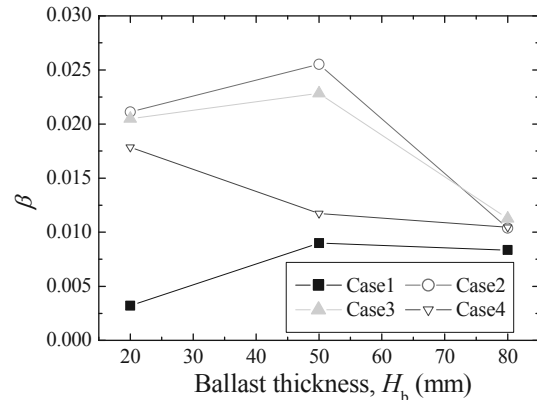


Figure 4. Relationships between gradual subsidence parameter β and ballast thickness H_b before tie-tamper implementation

Figure 4 shows the relationships between the gradual subsidence parameter β and ballast thickness H_b before tie-tamper implementation. It should be noted that 50 mm H_b was used to represent the 250 mm ballast thickness adopted for the standard design because the model size was at a scale of one-fifth. Interestingly, it is seen in the figure that β was highest when $H_b = 50$ mm in Cases 2 and 3. High β values indicate a substantial amount of gradual settlement; thus, these results suggest that the standard ballast thickness of 250 mm is ineffective for minimal settling.

The residual settlement characteristics were investigated in detail with PIV analysis. First, the displacement magnitude and direction of crushed stones and roadbeds induced by 100 cyclic loadings were estimated by analyzing consecutive digital images. The distributions of maximum shear strain γ_{max} generated in the crushed stones and roadbeds were next calculated. Figures 5 to 7 show the results obtained from Cases 1, 2, and 3. Results could not be obtained from Case 4 because the monotonic color of dark gray Natom sand resulted in ineffective pattern matching of PIV.

As shown in Fig. 5, a high value of γ_{max} was noted in Cases 1-1 and 1-2 until the ground depth reached the bottom steel plate. However, the concentration of γ_{max} could not be observed in Case 1-3 near the bottom steel plate. Similarly, the concentration of γ_{max} could not be observed in the roadbeds for Cases 2-3 and 3-3, as shown in Figs. 6 and 7. These results indicate that when $H_b = 80$ mm, γ_{max} can be sustained in

roadbeds, which can be explained by the limited distribution of stress applied by the footing with a width of 48 mm.

Except for the cases in which $H_b = 80$ mm, residual settling of the footing was attributed to total compression of crushed stones and roadbed materials. In general, stress concentration in roadbeds should be higher in the $H_b = 20$ mm cases than those in the $H_b = 50$ mm cases. Therefore, owing to the plastic deformation of roadbeds, the highest β value was observed in Case 4, in which $H_b = 20$ mm, as shown in Fig. 4.

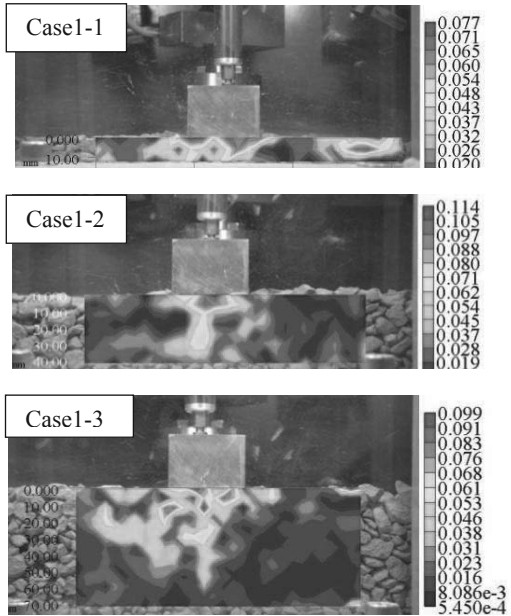


Figure 5. Distribution of maximum shear strain generated before tie-tamper implementation (Case 1)

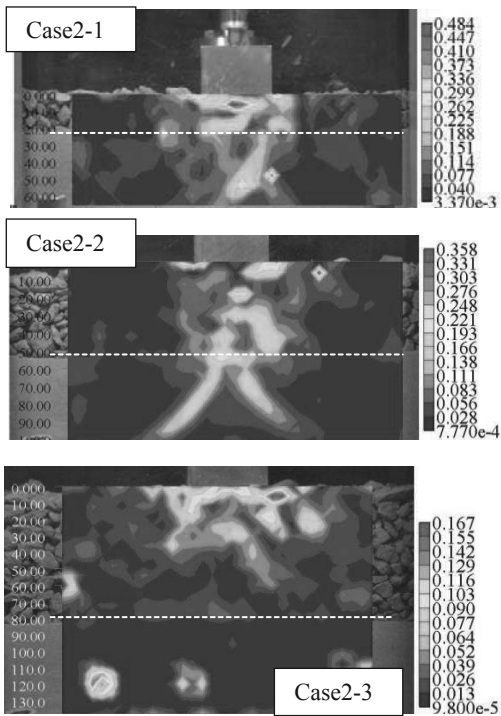


Figure 6. Distribution of maximum shear strain generated before tie-tamper implementation (Case 2)

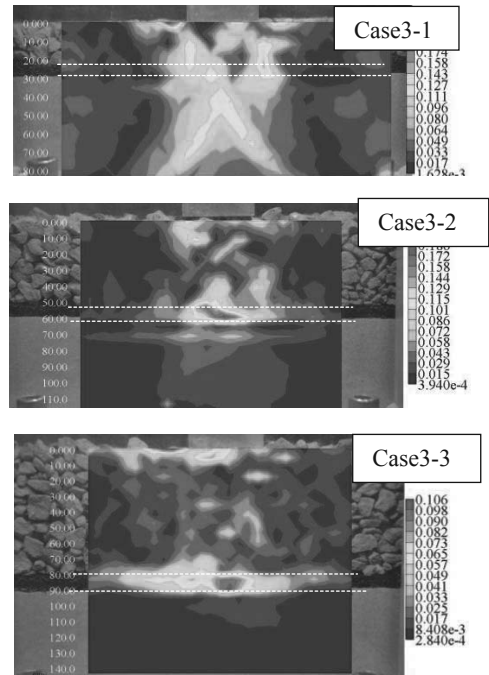


Figure 7. Distribution of maximum shear strain generated before tie-tamper implementation (Case 3)

Conversely, the compression of crushed stones was higher in the $H_b = 50$ mm cases than those in the $H_b = 20$ mm cases. If nonlinear compression of roadbeds is relatively moderate, the deformation modulus of the roadbeds changes slightly through the change in stress levels. In this situation, β can be higher in the $H_b = 50$ mm cases compared to that when $H_b = 20$ mm.

3.2 Effects of tie-tamper implementation

Figure 8 shows typical relationships between footing settlement and applied stress, represented by convex curves, in Case 1-1 when the 1st, 10th, and 100th cyclic loadings were applied before tie-tamper implementation. In this research, the curves were fitted by bilinear lines, and the slopes of the two lines were estimated as k_1 and k_2 . Displacement u_2 was estimated by dividing the applied stress by k_2 . The parameter u_2 decreased and tended to show a constant value in each case with an increase in the number of cyclic loadings (Fig. 9). Therefore, these constant values will be used in the following discussion.

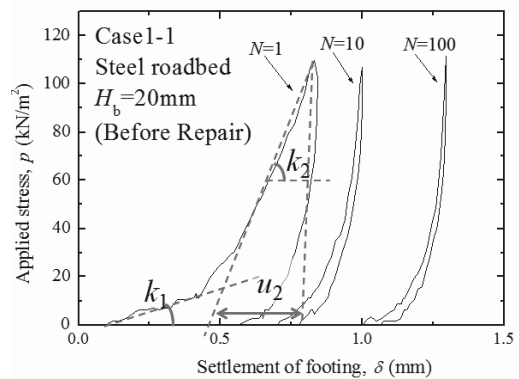


Figure 8. Relationships between footing settlement and applied stress in Case 1-1 before tie-tamper implementation

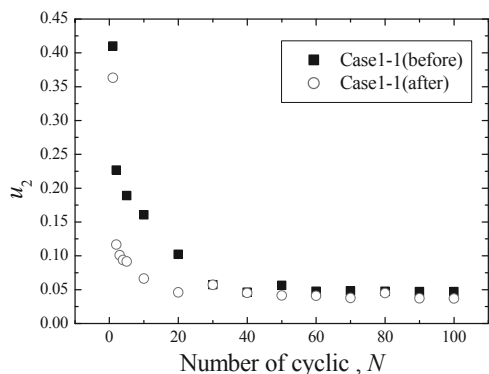


Figure 9. Relationships between displacement u_2 and number of cyclic loadings in Case 1-1 before and after tie-tamper implementation

Parameters u_2 , C , α , and β in Eq. 1 were evaluated from 100 cyclic loadings conducted before and after tie-tamper implementation. The relationships between u_2 and the remaining three parameters before and after tie-tamper implementation are shown in Figs. 10, 11, and 12.

Figure 10 shows that α were in the range 0.9–1.5 before tie-tamper implementation regardless of roadbed type and ballast thickness. Here, α represents the duration periods of the initial settlement process (Eq. 1). The figure also shows that α decreased more after tie-tamper implementation than that before. This tendency can be clearly observed when u_2 is higher, which indicates that the duration periods of the initial settlement process increased after tie-tamper implementation.

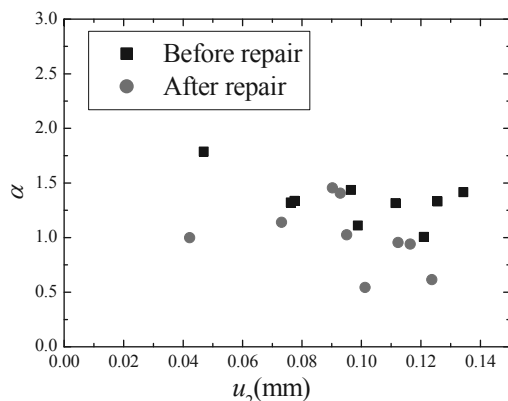


Figure 10. Relationships between displacement u_2 and duration periods of the initial settlement process α

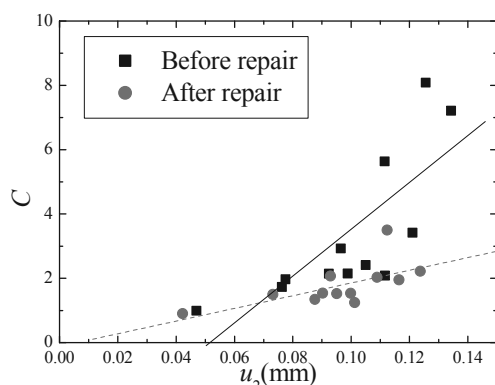


Figure 11. Relationships between displacement u_2 and amount of initial settlement C

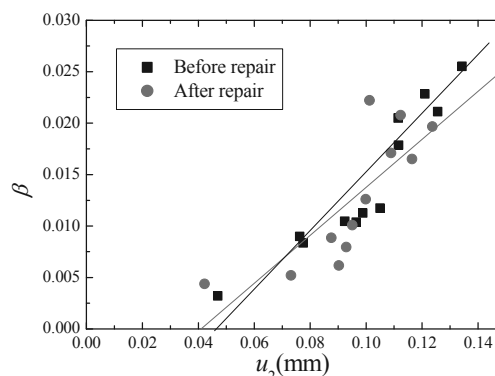


Figure 12. Relationships between displacement u_2 and degree of gradual settlement β

Parameters C and β proportionally increased with an increase in u_2 , as shown in Figs. 11 and 12. Here, C represents the amount of initial settlement, and β represents the degree of the gradual settlement. Figure 11 shows a higher decrease in C after tie-tamper implementation than that before. The same tendency was also clearly observed at higher u_2 because roadbeds became denser as a result of cyclic loadings; therefore, the amounts of initial settlement decreased after tie-tamper implementation. Conversely, Fig. 12 shows that β was nearly the same after tie-tamper implementation as that before. These results suggest that although the characteristics of the initial settlement process are significantly altered after tie-tamper repair, the degree of gradual subsidence is minimal regardless of ballast thickness and roadbed type.

4 CONCLUSION

The effects of ballast thickness and tie-tamper repair on the settlement characteristics of ballasted tracks were investigated by conducting a series of cyclic loading tests on model grounds. The following conclusions were derived from this research:

- (1) The standard 250 mm ballast thickness is ineffective for minimizing settlement, particularly when the nonlinearity of roadbed compressibility is relatively moderate.
- (2) The characteristics of the initial settlement process are altered considerably after tie-tamper implementation; however, the degree of gradual subsidence is minimal regardless of ballast thickness and roadbed type.

5 ACKNOWLEDGEMENTS

The authors would like to thank Mr. Kazunori Ito of the Railway Technical Research Institute for his assistance in conducting experiments.

6 REFERENCES

- Ishikawa, T. and Namura, A. 1995. Cyclic deformation characteristics of the railroad ballast in full scale tests, Journal of JSCE, No.512, 47-59 (in Japanese).
- Sekine, E., Ishikawa, T and Kouno, A. 2005. Effect of ballast thickness on cyclic plastic deformation of ballasted track, RTRI Report, Vol. 19, No.2, 17-22 (in Japanese).